Mon. Not. R. Astron. Soc. **000**, 000–000 (2007) Printed 5 February 2008 (MN LATEX style file v2.2)

The distant red galaxy neighbour population of $1 \leq z \leq 2$ QSOs and optically obscured sources*

Carlos G. Bornancini[1,2], Diego G. Lambas[1,3]
[1] *Grupo de Investigaciones en Astronomía Teórica y Experimental, IATE*
Observatorio Astronómico, Universidad Nacional de Córdoba
Laprida 854, X5000BGR, Córdoba, Argentina.
[2] *Secretaría de Ciencia y Técnica de la Universidad Nacional de Córdoba.*
[3] *Consejo Nacional de Investigaciones Científicas y Técnicas (CONICET), Avenida Rivadavia 1917, C1033AAJ, Buenos Aires, Argentina.*

arXiv:astro-ph/0702155v1 6 Feb 2007

5 February 2008

ABSTRACT

We study the Distant Red Galaxy (DRG, $J-K_s > 2.3$) neighbour population of Quasi Stellar Objects (QSOs) selected from the Sloan Digital Sky Survey (SDSS) in the redshift range $1 \leq z \leq 2$. We perform a similar analysis for optically obscured AGNs (i.e. with a limiting magnitude $I > 24$) detected in the mid-infrared (24 μm) with the Spitzer Space Telescope and a mean redshift $z \sim 2.2$ in the Flamingos Extragalactic Survey (FLAMEX). Both QSOs and obscured AGN target samples cover 4.7 deg^2 in the same region of the sky. We find a significant difference in the environment of these two target samples. Neighbouring galaxies close to QSOs tend to be bluer than galaxies in optically obscured source environments. We also present results on the cross–correlation function of DRGs around QSOs and optically faint mid-infrared sources. The corresponding correlation length obtained for the QSO sample targets is r_0=5.4 ± 1.6 Mpc h^{-1} and a slope of γ=1.94 ± 0.10 . For the optically obscured galaxy sample we find r_0=8.9 ± 1.4 Mpc h^{-1} and a slope of γ=2.27 ± 0.20. These results indicate that optically faint obscured sources are located in denser environment of evolved red galaxies compare to QSOs.

Key words: cosmology: large-scale structure of Universe–galaxies: galaxies: high-redshift–quasars: general

1 INTRODUCTION

Studies of large samples of distant galaxies are fundamental to provide a deeper insight in the formation and evolution of galaxies and systems of galaxies, such as clusters and groups. Using measurements of galaxy clustering at $z \sim 1-2$ one can test the predictions of cosmological models of structure formation and evolution (Kauffmann et al. 1999). In the last years diverse photometric selection techniques have been developed in order to select high redshift galaxies. In particular the Lyman break technique is an ideal method for selecting a large number of distant galaxies and for studying the large-scale distribution and properties of star-forming systems at high redshifts from multicolour optical data (Steidel et al. 1996; Madau et al. 1996) . This technique requires a high rest-frame far ultraviolet luminosity, and so will preferentially select galaxies with recent or unobscured active star-formation (Steidel et al. 1999). A new near-infrared selection technique has been developed in recent years to select samples of galaxies at high redshifts. The Distant Red Galaxies (DRGs, hereafter) colour–cut criterion ($J-K_s > 2.3$, Vega system) (Saracco et al. 2001; Franx et al. 2003; van Dokkum et al. 2003) is expected to select galaxies with prominent rest frame optical breaks, caused by the 3625 Å Balmer-break or the 4000 Å Ca II H+K break. The Balmer discontinuity at 3625 Å is strongest in A-type stars and the 4000 Å break is characteristic of coolers stars with types later than G0 and strong in giant and supergiant stars (Förster Schreiber et al. 2004). van Dokkum et al. (2003) found that the DRG criterion selects galaxies with rest-frame optical colours similar to those of normal nearby galaxies. Using deep mid-infrared observations with IRAC on the Spitzer Space Telescope,

---

* Based on observations and/or data products by the Flamingos Extragalactic Survey. FLAMINGOS was designed and constructed by the IR instrumentation group (PI: R. Elston) at the University of Florida, Department of Astronomy, with support from NSF grant AST97-31180 and Kitt Peak National Observatory

Labbé et al. (2005) found that 70% of the DRGs are best described by dust-reddened star forming models and 30% are very well fit with old stellar population, passive star evolution galaxy models. By comparison of the stellar populations of DGRs to those obtain in Lyman-break galaxies (LBGs), Labbé et al. (2005) found that the average mass-to light ratios (M/L_K) of the DRGs are about three times higher than the LBGs sample, indicating that DGRs may represent massive and old galaxies, similar to those found in the local Universe. A similar study by Förster Schreiber et al. (2004) comparing LBGs and DRGs at similar redshifts and rest-frame V-band luminosities, shows that DRGs are older, more massive and more obscured for any given star formation history than LBGs. Recent works by Conselice et al. (2006) and Grazian et al. (2006a) show that this single near IR colour–cut selects a rather heterogeneous sample of galaxies, from distant luminous massive systems, to a significant fraction of less luminous dusty star-burst and galaxies with mixed morphology at redshifts $z \sim 2$, with extended tails at $z = 1$ and $z = 4$.

At low redshifts, QSO environments show similar characteristics of those found in normal galaxies (Smith et al. 1995; Coldwell & Lambas 2006). Moreover, Smith et al. (1995) found that the cross-correlation function between low ($z < 0.3$) QSOs and galaxies, is consistent with the auto-correlation function of galaxies selected from the APM Galaxy Survey. Unlike radio-loud QSOs, Ellingson et al. (1991) found that radio-quiet QSOs at $0.3 < z < 0.6$ are rarely found in high density environments as rich as Abell class 1. Recently, Serber et al. (2006) studying the environment of $z < 0.4$ luminous ($M_i < -22$) quasars in the SDSS area, found that they are located in higher local overdensity regions than are typical L^* galaxies. However, the results for QSO environment at higher redshifts ($1 \leq z \leq 2$) are contradictory. Yee & Green (1987) found that some of the $z \sim 0.6$ QSOs are located in environments as rich as those of Abell class 1 clusters. Hall & Green (1998) reported a significant excess of faint galaxies in the fields of $z = 1 - 2$ quasars. No excess galaxy population associated with radio-quiet QSOs are reported by Boyle & Couch (1993) at $z \sim 1$. Croom & Shanks (1999) found an anti-correlation between radio-quiet QSOs and galaxies at redshifts $z \sim 1 - 1.5$. Coil et al. (2006) studied the clustering of galaxies around a sample of $0.7 < z < 1.4$ QSOs selected from the SDSS and DEEP2 surveys. They found, from a two-point cross-correlation analysis, that the local environment of QSOs is consistent with the mean environment of the full DEEP2 galaxy population and that they cluster similar to the blue, star-forming galaxies rather than the red galaxies. Their results imply that high redshift QSOs do not reside in particularly massive dark matter halos.

Using the DRGs criterion, Kajisawa et al. (2006) reported a discovery of proto-clusters candidates around 6 high redshifts radio galaxies at $z \sim 2.5$ on the basis of excess of $J - K_s$ colour–selected galaxies. Recently, a similar colour criterion was adopted to identify and to study the environment of very distant objects. This method uses a colour cut $i_{775} - z_{850} > 1.3$ which select objects at $z \sim 6$. An overdensity of galaxies around the most distant radio–loud QSO (SDSS J0836+0054 at $z = 5.8$) was reported by Zheng et al. (2006), who found a surface density six times higher than the number expected from deep fields at similar redshifts. Stiavelli et al. (2005) found an excess of $i_{775} - z_{850} > 1.3$ galaxies around one of the most distant QSOs at $z = 6.28$.

In this paper we investigate the population and colour distribution of DRGs, selected at bright near–IR magnitudes ($K_s < 19.5$, Vega system) around high redshift QSOs ($1 \leq z \leq 2$) and optical obscured sources ($z \sim 2.2$) in the FLAMINGOS Extragalactic Survey (FLAMEX, Elston et al. (2006)).

This paper is organised as follows: Section 2 describes the sample analysed, The DRG number counts are analysed in Section 3. In Section 4 we study the colour distribution of galaxies in different environments. We investigate the QSO–DRGs and Obscured–DRGs cross-correlation analysis in Section 5. Finally we discuss our results in Section 6.

In this work we assume a standard ΛCDM model Universe with cosmological parameters, Ω_M=0.3, Ω_Λ=0.7 and a Hubble constant of H_0 =100 Km s^{-1}Mpc^{-1}. All magnitudes are expressed in the Vega system.

2 OBSERVATIONAL SAMPLE

The FLAMINGOS Extragalactic Survey (FLAMEX, Elston et al. (2006)) is a wide-area, near-infrared imaging survey in J and K_s bands within the NOAO Deep Wide-Field Survey (NDWFS) regions (Jannuzi & Dey 1999). This paper uses catalogues of the first Data Release DR1 of the northern part of the Survey (Boötes field) that covers 4.7 deg^2 in both J and K_s bands [1]. Using Monte Carlo simulations Elston et al. (2006) found that more than 90 % of the survey region is complete to $K_s = 19.2$, with 50 % being complete to $K_s = 19.5$. A detailed description of the observing strategy and data reduction can be found in Elston et al. (2006). The catalogues were made using K_s–selected objects for each survey subset with the SExtractor package (Bertin & Arnouts 1996), using dual image mode to measure the J–band magnitudes within the same regions. Detections in the different bands were matched if the centroids were within 1 $''$ of each other. $J - K_s$ colours were calculated using $4''$ diameter aperture photometry, sufficiently large to avoid intrinsic aberrations that cause the PSF to vary significantly across the field and to produce robust photometry across entire subfields.

In order to reject spurious objects lying in the edges of the images, we selected objects that not overlap with another object using the SExtractor parameters `FLAGS` = `0` and `WEIGHT_MAP` < 0.7, in both J and K_s bands.

For two different reasons, no star-galaxy separation was performed. First, the variable PSF in the FLAMEX area precluded use of structural information to separate stars from extended sources and second, DRGs are of such small apparent size that considerable fraction of them would possibly be misclassified as stars and rejected from the final catalogues. As noted by Elston et al. (2006), and as can be seen in the colour-magnitude diagram (Figure 1), the $J - K_s$ colours alone provides a simple means of performing star-galaxy separation. The two horizontal sequences at $J - K_s$=0.4 and $J - K_s$=0.8 correspond to galactic stars with types later than G5 and earlier than K5, respectively

---

[1] http://flamingos.astro.ufl.edu/extragalactic/

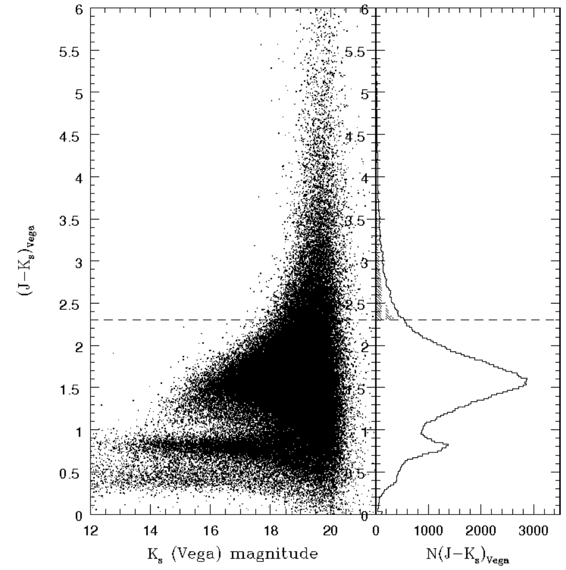

Figure 1. Left panel: $J - K_s >$ vs K_s (Vega) colour-magnitude diagram for the FLAMEX field (Boötes area). Right panel: Colour distribution. Dashed lines show the DRGs criterion adopted.

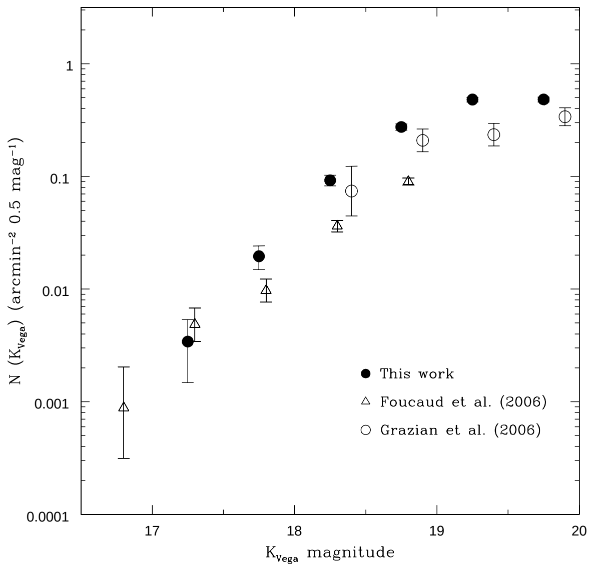

Figure 2. Differential number counts as a function of K_s magnitude for the DRG sample (Filled circles). The error bars plotted represent Poissonian errors (3 σ). We include the DRG number counts obtained in the literature. Open triangles represent data from the UKIDSS Ultra Deep Survey Early Data Release (Foucaud et al. 2006, private communication) and open circles are data obtained in the GOODS-MUSIC Sample, Grazian et al. (2006a).

(Finlator et al. 2000). Red galaxies with $J - K_s$ >2.3 are well separated from stars. We also show in Figure 1 the DRGs criterion adopted (Dashed lines). Our final catalogue consist of 7131 DRGs in a contiguous area of 4.7 degree^2, representing the largest sample of DRGs selected at bright magnitudes $K_s < 19.5$.

The QSO sample analysed in this work was obtained using the NED Database. [2] We selected QSOs in the redshift range $1 \leq z \leq 2$ in the FLAMEX area. The sample consists of twelve QSOs selected from the Sloan Digital Sky Survey (SDSS, Data Release 1 to 4) (York et al. 2000; Richards et al. 2002) and one X–ray selected AGN (Puchnarewicz et al. 1997) (See Table 2).

We also choose a sample of optically obscured galaxies discovered with the Spitzer Space Telescope, which are either optically very faint (R >24.5) or invisible (R >26) with no counterparts in the NOAO Deep Wide-Field Survey regions. The main goal of this survey is to select optically very faint galaxies but bright enough in the mid-infrared for redshift determination with the Infrared Spectrograph on Spitzer (IRS), which would not have been identified in previous optical studies. Sources with $I > 24$ mag were identified with the Multi-band Imaging Photometer (MIPS) on the Spitzer Space Telescope to a limiting 24 μm flux density above 0.75 mJy. 114 sources of the total sample met this optical criterion. Out of these, 17 sources have no optical or have very faint optical counterparts. Rejecting sources lying in the edges of the images, where noise level are high and signal to noise values are low, we finally selected 6 sources located within the FLAMEX area, with a mean redshift distribution $z \sim 2.2$. The redshift range of the selected sources are similar to that of the redshift distribution of DRGs with $K_s < 20.15$ (Vega magnitudes) found by Grazian et al. (2006a). Redshifts from this sample were derived primarily from strong silicate absorption features (Houck et al. 2005). We also selected another two sources with feasible redshift determinations derived by a weak silicate absorption feature, based on fits of redshifted spectral templates of local Ultraluminous Infrared Galaxies (ULIRGS) from Weedman et al. (2006). Full details of the sample selection and redshift determination is given in Houck et al. (2005); Weedman et al. (2006).

As noted by Houck et al. (2005) template fits suggest that most of the optically obscured sources are dominated by an AGN component, i.e. a steeply rising spectra and varying levels of silicate absorption, similar to the infrared spectra of known local AGNs. By comparing bolometric luminosities of submillimeter selected galaxies, such as those detected in SCUBA or MAMBO suryeys, Houck et al. (2005) found that the obscured source sample seems to represent sources that have a hotter dust component than typical submillimeter-selected galaxies, assuming that mid-infrared luminosities scale to bolometric luminosities similar than in template sources which fit the mid-infrared spectra. Using this scaling, the obscured sources have implied infrared luminosities between 6×10^{12} $L_{\odot}$ and 6×10^{13} $L_{\odot}$, similar to bright QSOs at $z \sim 2$ (Hopkins et al. 2005).

3 GALAXY NUMBER COUNTS

We have computed the differential number counts of DRGs per unit area as a function of K_s magnitude which are shown in Figure 2. We use SExtractor `MAG_AUTO` magnitudes for this calculation and estimate error bars using

---

[2] http://nedwww.ipac.caltech.edu/ - the NASA-IPAC Extragalactic Database

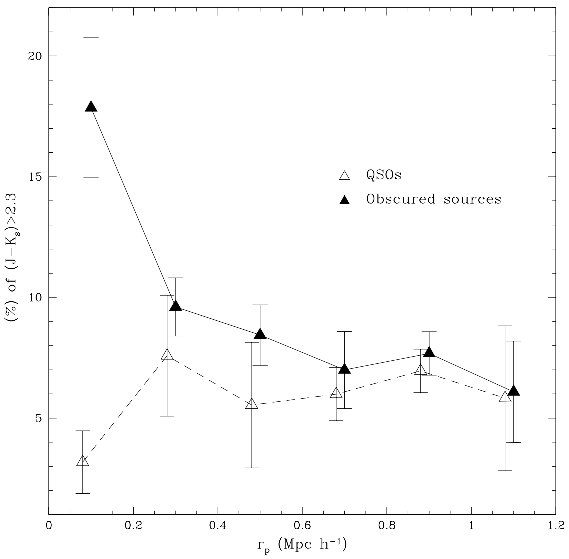

Figure 3. Percentage of galaxies with $J - K_s > 2.3$ vs projected distance for QSOs (Open triangles) and optically obscured galaxies (Filled triangles). Error bars were estimated using jackknife re–sampling techniques.

3 σ uncertainties estimated using Poissonian errors of the raw galaxy counts (See Table 1). We compare our determinations with $K-$band number counts for DRGs obtained by Grazian et al. (2006a) in the GOODS–MUSIC Sample and with estimates obtained in the UKIDSS Ultra Deep Survey Early Data Release (Foucaud et al. 2006, private communication). We have done this comparison using Vega magnitudes, assuming a transformation $K_{Vega} = K_{AB} - 1.85$ (Cool et al. 2006). For K_s >17.5 our counts are systematically higher than those obtain by Foucaud et al. This discrepancy can be explained by cosmic variance because of the small area (0.62 deg^2) of the Early Data Release of the UKIDSS Ultra Deep Survey.

Table 1. DRG number counts as a function of K_s band. The columns give the central bin magnitude, the raw counts, counts in units of arcmin^{-2}mag^{-1} and 3 σ uncertainties estimated using Poissonian errors.

(1) *bin*	(2) N	(3) log(Σ) arcmin^{-2}mag^{-1}	(4) Error (3σ)
17.25	28	−2.466	0.0019
17.75	160	−1.709	0.0046
18.25	756	−1.035	0.0100
18.75	2248	−0.561	0.0173
19.25	3939	−0.318	0.0229
19.75	3944	−0.317	0.0230

4 COLOUR DISTRIBUTION OF GALAXIES AROUND QSOS AND OPTICALLY OBSCURED SOURCES

In order to study the neighbour population of galaxies in these environments, we calculate the colour distribution of neighbouring galaxies according to the different target distances. In Figure 3, we can see the percentage of DRGs respect to $15.5 < K_s < 19.5$ galaxies vs projected distance for two different target samples. QSO targets are represented with open triangles and optically obscured galaxies are represent with filled triangles. Error bars were estimated using $jackknife$ re–sampling techniques (Efron 1982). As can be seen, in the vicinity of these targets ($r < 0.3$ Mpc h^{-1}) the distribution of colours of galaxies is significantly different. Neighbouring galaxies close to QSOs tend to be bluer than galaxies in optically obscured source environments. For these objects, the fraction of galaxies with $J - K_s > 2.3$ decreases from 20% to 5%.

5 QSO-DRGS AND OBSCURED-DRGS CROSS-CORRELATION ANALYSIS

In this section we analyse the relative spatial clustering of DRGs and QSOs and optically obscured galaxies. In order to obtain the cross–correlation length r_0, we first determine the projected cross–correlation function using QSOs as targets and the DRG population in their fields as tracer galaxies. We have done the same computation using optically obscured galaxies as targets and DRGs as tracer galaxies.

We use the Peebles estimator (Peebles 1980) of the projected cross-correlation function:

$$\omega(\sigma) = \frac{n_R}{n_G}\frac{QG(\sigma)}{QR(\sigma)} - 1, \qquad (1)$$

where n_G and n_R are the numbers of DRGs in the sample and in a random sample respectively, $QG(\sigma)$ is the number of real QSO-DRGs (or OBS-DRGs, using obscured galaxy targets) pairs separated by a projected distance in the range σ, $\sigma + \delta\sigma$, and $QR(\sigma)$ are the corresponding pairs when considering the random galaxy sample.

We have estimated the cross-correlation length taking into account the selection function of the galaxy survey as a function of the distance to the targets (QSOs or optically obscured galaxies, respectively). Assuming a power-law model for the real space cross correlation function it is found:

$$\omega(\sigma) = B\sqrt{\pi}\frac{\Gamma\left[(\gamma-1)/2\right]}{\Gamma(\gamma/2)}\frac{r_0^{\gamma}}{\sigma^{\gamma-1}}, \qquad (2)$$

where the constant B depends on the differences of the selection function of the different targets and tracers.

When the distance of these targets are known, the constant B is given by (Lilje & Efstathiou 1988):

$$B = \frac{\sum_i N(y_i)}{\sum_i \frac{1}{y_i^2}\int_0^{\infty} N(x)x^2dx}, \qquad (3)$$

where $N(y_i)$ is the selection function of the galaxy survey, y_i is the distance to target i and the sum extends over all QSO (or obscured source) targets in the sample.

We model the selection function using the distance distribution of DRGs in the GOODS Survey ((Grazian et al.

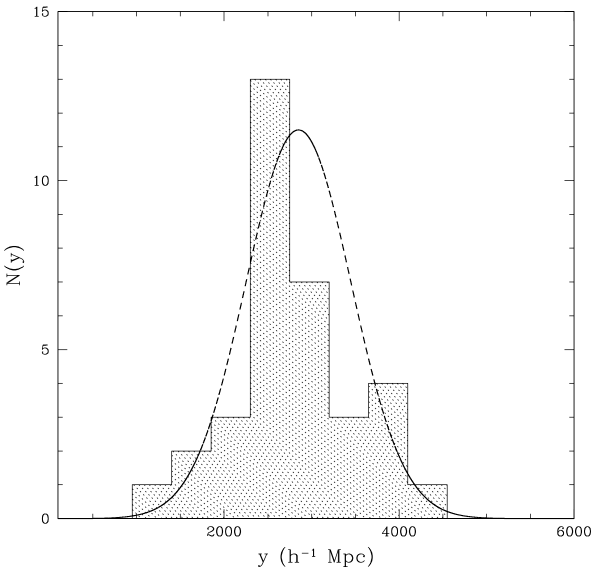

Figure 4. Distance distribution of $K_s < 19.5$ DRGs selected from the GOODS survey (Grazian et al. 2006a) with photometric redshift measurements. Dashed lines shows the selection function obtained by fitting a Gaussian function.

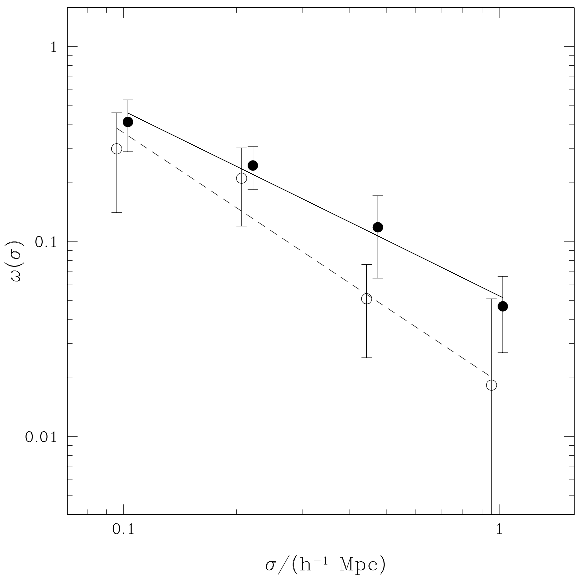

Figure 5. Projected cross–correlation function between QSOs and DRGs in the redshift range $1 \leq z \leq 2$ (Filled circles) and between optically obscured galaxies with $z \sim 2.2$ and DRGs with $K_s < 19.5$ (Open circles). Error bars correspond to 1 σ uncertainty estimated using the jackknife technique (Efron 1982).

2006b)) for galaxies with photometric redshifts and K_s magnitudes < 19.5. We convert measured redshifts to comoving distances along the line of sight assuming a flat ΛCDM model Universe with the same parameters quoted in the Introduction. In Figure 4 we show the distance distribution of DRGs in the GOODS area with $K_s < 19.5$ and with photometric redshift determinations. We model the distance distribution with a Gaussian function centred at y=2850 Mpc h^{-1} and with a standard deviation of σ_y= 600 Mpc h^{-1}.

In Figure 5 we show the obtained projected cross–correlation function between QSOs and DRGs in the redshift range $1 \leq z \leq 2$ (Filled circles) and between optically obscured galaxies with $z \sim 2.2$ and DRGs with $K_s < 19.5$ (open circles). The error bars were estimated using the *jackknife* technique (Efron 1982). The corresponding cross–correlation length derived for the QSO sample targets is r_0=5.4 ± 1.6 Mpc h^{-1} and a slope of γ=1.94 ± 0.10. Using the optically obscured galaxy sample as targets we find r_0=8.9 ± 1.4 Mpc h^{-1} and a slope of γ=2.27 ± 0.20. We tested the accuracy of this result by varying the $N(y_i)$ distribution over a reasonable range of values for $\bar{y}$ and σ_y. We find that the calculated r_0 is only weakly dependent on the $\bar{y}$ used, and is only affected at the 10% level.

6 SUMMARY AND DISCUSSIONS

We have analysed the QSOs and optically obscured sources environment using the DRG photometric technique ($J - K_s > 2.3$). The sample of QSOs at $1 \leq z \leq 2$ were selected from the Sloan Digital Sky Survey and the optically faint sources sample were detected in the mid-infrared with the Spitzer Space Telescope at z∼ 2.2 in the Flamingos Extragalactic Survey (FLAMEX). We find that there are significant differences in the environment and galaxy properties around these two different targets. We find that neighbouring galaxies next to QSOs tend to be bluer than galaxies in optically obscured source environments. The fraction of galaxies with $J - K_s > 2.3$ in the vicinity ($r_p < 0.3$ Mpc h^{-1}) of optically obscured sources decreases from 20% to 5%. These results are consistent with those of Coil et al. (2006) who find that the local environment of $0.7 < z < 1.4$ QSOs (using the 3^{rd}–nearest–neighbour surface density of surrounding DEEP2 galaxies) has a similar overdensity than that of blue galaxies, differing from red galaxy population at 2σ significance. We also present results on the cross–correlation function of DRGs around QSOs and optically obscured sources. The corresponding cross–correlation length derived for the QSO and the DRGs is r_0=5.4 ± 1.6 Mpc h^{-1} with a slope of γ=1.94 ± 0.10. Using the optically obscured galaxy sample as targets we find r_0=8.9 ± 1.4 Mpc h^{-1} and a slope of γ=2.27 ± 0.20. We point out that the results of Sections 4 and 5 consistently indicate that obscured sources are located in higher density environment compared to QSOs, as shown by both, the colour distribution and the cross-correlation analysis.

It is possible that the optically obscured sources population are not rare objects. Using a QSO sample in the full Boötes field, Weedman et al. (2006) found that unobscured, classical type 1 QSOs and optically obscured sources with similar redshifts are similar in number. As noted by Weedman et al. (2006), sources selected at 24 μm, which are optically faint, are dominated by dusty sources with spectroscopic indicators of an obscured AGN rather than a starburst. Houck et al. (2005) found that these sources represent ULIRGS powered by a AGN and they have bolometric luminosities exceeding 10^{13} M$\odot$, if bolometric luminosities scale with mid–infrared luminosities as in the templates which fits the spectra. This value is similar to those found for bright

QSOs at $z \sim 2$ (Hopkins et al. 2005). Ellingson et al. (1991) have showed that luminous QSOs in rich galaxy cluster environments evolves much more quickly than those in poor environments which are present at all redshifts. It is possible that the QSO activity in optical obscured sources have vanished as a consequence of the rich environment where they are located or the luminous central engine is heavily obscured by the dust.

Few studies exists in the Literature about the spatial clustering of DRGs. Foucaud et al. (2004) found a large correlation length of $r_0 \sim 12\ h^{-1}$ Mpc for a sample of bright DRGs (K_{AB} ~20.7, or K_{Vega}~ 18.8) in a small area of the Early data release of the UKIDSS survey. Grazian et al. (2006a) found $r_0 = 7.41^{+3.45}_{-4.84}\ h^{-1}$ Mpc for DRGs with $1 < z < 2$ and $K_{AB} < 22$ ($K_{Vega} < 20$). The larger correlation length found by Foucaud et al. (2004) could be interpreted as evidence for luminosity segregation, where the most luminous DRGs are more strongly clustered. If we compare our values obtained in the cross-correlation function analysis with the mean value obtained for the DRGs in the field by Grazian et al. (2006a), our results suggest that the sample of unobscured QSOs at high redshift analysed tend to be located in typical environment of DRGs with a transient phase in the evolution of normal galaxies. However, our cross-correlation results indicate that optically obscured sources probably represent massive galaxies located in rich environment of DRGs at high redshifts.

7 ACKNOWLEDGEMENTS

We are thankful to the referee Dr. Michael Strauss for his careful reading of the manuscript and a number of comments, which improved the paper.

This paper used public catalogues form the Flamingos Extragalactic Survey, with support from NSF grant AST97-31180 and Kitt Peak National Observatory This work was partially supported by the Consejo Nacional de Investigaciones Científicas y Técnicas (CONICET) and the Secretaría de Ciencia y Técnica de la Universidad Nacional de Córdoba.

This research has made use of the NASA/IPAC Extragalactic Database (NED), which is operated by the Jet Propulsion Laboratory, California Institute of Technology, under contract with the National Aeronautics and Space Administration.

Funding for the SDSS and SDSS-II has been provided by the Alfred P. Sloan Foundation, the Participating Institutions, the National Science Foundation, the U.S. Department of Energy, the National Aeronautics and Space Administration, the Japanese Monbukagakusho, the Max Planck Society, and the Higher Education Funding Council for England. The SDSS Web Site is http://www.sdss.org/. The SDSS is managed by the Astrophysical Research Consortium for the Participating Institutions. The Participating Institutions are the American Museum of Natural History, Astrophysical Institute Potsdam, University of Basel, Cambridge University, Case Western Reserve University, University of Chicago, Drexel University, Fermilab, the Institute for Advanced Study, the Japan Participation Group, Johns Hopkins University, the Joint Institute for Nuclear Astrophysics, the Kavli Institute for Particle Astrophysics and Cosmology, the Korean Scientist Group, the Chinese Academy of Sciences (LAMOST), Los Alamos National Laboratory, the Max-Planck-Institute for Astronomy (MPIA), The Max-Planck-Institute for Astrophysics (MPA), New Mexico State University, Ohio State University, University of Pittsburgh, University of Portsmouth, Princeton University, the United States Naval Observatory, and the University of Washington.

REFERENCES

Bertin, E., & Arnouts, S. 1996, *A&AS*, 117, 393

Boyle, B. J., & Couch, W. J. 1993, *MNRAS*, 264, 604

Coil et al. ApJ letters, in press

Coldwell, G. V., & Lambas, D. G. 2006, *MNRAS*, 371, 786

Conselice et al. ApJ letters, in press

Cool, R. J., et al. 2006, *AJ*, 132, 823

Croom, S. M., & Shanks, T. 1999, *MNRAS*, 303, 411

Ellingson, E., Yee, H. K. C., & Green, R. F. 1991, *ApJ*, 371, 49

Elston, R. J., et al. 2006, *ApJ*, 639, 816

Efron, B., 1982, The Jackknife, the Bootstrap and Other Resampling Plans, Philadelphia: SIAM.

Finlator, K., et al. 2000, *AJ*, 120, 2615

Förster Schreiber, N. M., et al. 2004, *ApJ*, 616, 40

Foucaud et al. 2006, *MNRAS*, submitted

Franx, M., et al. 2003, *ApJ*, 587, L79

Hall, P. B., & Green, R. F. 1998, *ApJ*, 507, 558

Grazian, A., et al. 2006a, *A&A*, 449, 951

Grazian, A., et al. 2006b, *A&A*, 453, 507

Hopkins, P. F., Richards, G. T., & Hernquist, L., 2006, ApJ submitted, astro-ph/0605678

Houck, J. R., et al. 2005, *ApJ*, 622, L105

Jannuzi, B. T., & Dey, A., 1999, in ASP Conf. Ser. 191, Photometric Redshifts and Detection of High Redshifts Galaxies, ed. R. Weynmann, L. Storrie Lombardi, M. Sawicki, & R. Brunner (San Francisco; ASP), 111-117

Kajisawa, M., Kodama, T., Tanaka, I., Yamada, T., & Bower, R. 2006, *MNRAS*, 371, 577

Kauffmann, G., Colberg, J. M., Diaferio, A., & White, S. D. M. 1999, *MNRAS*, 307, 529

Labbé, I., et al. 2005, *ApJ*, 624, L81

Lilje, P. B., & Efstathiou, G. 1988, *MNRAS*, 231, 635

Madau, P., Ferguson, H. C., Dickinson, M. E., Giavalisco, M., Steidel, C. C., & Fruchter, A. 1996, *MNRAS*, 283, 1388

Peebles, P. J. E., 1980, "The Large-Scale Structure of the Universe", Princeton University Press.

Puchnarewicz, E. M., et al. 1997, *MNRAS*, 291, 177

Richards, G. T., et al. 2002, *AJ*, 123, 2945

Saracco, P., Giallongo, E., Cristiani, S., D'Odorico, S., Fontana, A., Iovino, A., Poli, F., & Vanzella, E. 2001, *A&A*, 375, 1

Serber, W., Bahcall, N., Ménard, B., & Richards, G. 2006, *ApJ*, 643, 68

Smith, R. J., Boyle, B. J., & Maddox, S. J. 1995, *MNRAS*, 277, 270

Steidel, C. C., Giavalisco, M., Pettini, M., Dickinson, M., & Adelberger, K. L. 1996, *ApJ*, 462, L17

Steidel, C. C., Adelberger, K. L., Giavalisco, M., Dickinson, M., & Pettini, M. 1999, *ApJ*, 519, 1

Stiavelli, M., et al. 2005, *ApJ*, 622, L1
van Dokkum, P. G., et al. 2003, *ApJ*, 587, L83
Weedman, D. W., Le Floc'h, E., Higdon, S. J. U., Higdon, J. L., & Houck, J. R. 2006, *ApJ*, 638, 613
Yee, H. K. C., & Green, R. F. 1987, *ApJ*, 319, 28
York, D. G., et al. 2000, *AJ*, 120, 1579
Zheng, W., et al. 2006, *ApJ*, 640, 574

(1) Name	(2) redshift
SST24 1435203.99+330706.8	2.59±0.34
SST24 J142804.12+332135.2	2.34±0.28
SST24 J143358.00+332607.1	1.96±0.34
SST24 J143001.91+334538.4	2.46±0.20
SST24 J143251.82+333536.3	1.78±0.14
SST24 J143520.75+340418.2	2.08±0.21
SST24 J143026.05+331516.4	1.90*
SST24 J143429.56+343633.1	2.00*

Table 2. Optically obscured sources sample characteristics. SST24 source name derives from discovery with the MIPS 24 μm images, redshifts derived from strong (* weak) silicate absorption features.

(1) Name	(2) redshift
SDSS J143106.78+340910.9	1.098000
SDSS J143132.13+341417.3	1.039840
SDSS J143331.80+341532.8	0.957354
SDSS J143421.33+340446.9	1.956500
SDSS J142912.88+340959.1	2.229540
SDSS J143307.89+342315.9	1.950550
SDSS J143201.75+343526.2	1.070690
RIXOS F110–50	1.335000
SDSS J142744.44+333828.7	1.237000
SDSS J143605.08+334242.6	1.983830
SDSS J143628.09+335524.3	0.903084
SDSS J143543.72+342906.4	2.547330
SDSS J143627.79+343416.8	1.883490

Table 3. QSOs sample characteristics. Designation in IAU format and spectroscopic redshift.